

larger than the source dimension (L). For $\langle l \rangle \sim L$, the v_1 integration can be carried out using Bessel functions. The net result can still be approximated by this factor.

⁹For our geometry, the average scattering angle from the second particle in the front lobe ($x_{12} > 0$) is about 45° , and that in the back lobe ($x_{12} < 0$) about 135° . The intensity weighting factors for the Rayleigh-Gans particles are determined from H. H. Denman, W. Heller, and W. J. Pangonis, *Angular Scattering Functions for Spheres* (Wayne State Univ. Press, Detroit, Mich., 1966).

¹⁰H. C. Kelly, *J. Phys. A* **6**, 353 (1973).

¹¹B. Crosignani, P. Di Porto, and M. Bertolotti, in *Statistical Properties of Scattered Light* (Academic, New York, 1975).

¹²P. C. Colby, L. M. Narducci, V. Blumel, and J. Baer, *Phys. Rev. A* **12**, 1530 (1975).

¹³D. W. Oxtoby and W. M. Gelbart, *J. Chem. Phys.* **60**, 3359 (1974).

¹⁴L. A. Reith and H. L. Swimney, *Phys. Rev. A* **12**, 1094 (1975).

¹⁵A. J. Bray and R. F. Chang, *Phys. Rev. A* **12**, 2594 (1975).

¹⁶D. Beysens and G. Zalczner, *Phys. Rev. A* **15**, 765 (1977).

Anomalous Slowing of a Perpendicularly Injected Ion Beam in Both Quasilinear and Trapping Regimes

Masaaki Yamada and Steven W. Seiler

Plasma Physics Laboratory, Princeton University, Princeton, New Jersey 08540

(Received 24 June 1977)

The anomalous slowing of an ion beam injected perpendicularly to the confining magnetic field of a low- β plasma is experimentally verified in the nonlinear stages of the excited lower-hybrid instability. Furthermore, a transition of the main nonlinear mechanism from the quasilinear to the particle-trapping regime is demonstrated by varying beam parameters.

The ion distribution resulting from neutral- and/or ion-beam injection perpendicular to the confining magnetic field of a low- β plasma is theoretically predicted to destabilize microinstabilities,¹⁻³ and the injected beam is expected to lose its momentum anomalously fast as a result of wave-particle interaction.⁴ We wish to present the first experimental verification, to our knowledge, of anomalous slowing and velocity-space diffusion of a perpendicularly injected ion beam due to the nonlinear interaction of the beam with the excited lower-hybrid instability.

Two major nonlinear wave-particle interactions—particle trapping in a coherent wave trough^{5,6} or quasilinear velocity-space diffusion in a broad spectrum of waves^{7,8}—have been separately invoked as the saturation mechanisms of beam-driven plasma instabilities. In addition to the observed anomalous slowing, another novel contribution of the present experiment is that a transition of the nonlinear mechanism from the quasilinear to the particle-trapping regime is observed together with time-resolved measurements of the beam's velocity-space modification.

The experiments were performed in the thermally ionized potassium plasma of the Princeton University Q-1 device^{3,9} ($n_0 \approx 10^9 \text{ cm}^{-3}$; $T_e \leq T_i \approx 0.35 \text{ eV}$), with use of the machine layout in which the lower-hybrid wave, excited by spiral

ion-beam injection, had been identified by the wave's dispersion relation $\omega_r(\vec{k})$, where $\omega = \omega_r + i\gamma$ is the complex angular frequency, and \vec{k} the wave number.³ To follow the nonlinear evolution of the instability, a pulsed ion beam ($E_b = 0-100 \text{ eV}$; $0.001 \leq n_b/n_0 \leq 0.1$; $T_b = 0.5 \text{ eV}$) is used in the present experiment; the beam follows a helical path ($r_{\text{helix}} \approx 5\rho_i$, with ρ_i the target ion Larmor radius) and creates a double-humped ion velocity distribution [$f(v_1)$] in a cylindrical shell of the target plasma column ($r_{\text{column}} \approx r_{\text{helix}}$). A flute-type ($k_z \approx 0$; $\hat{z} \parallel \vec{B}_0$) lower-hybrid instability^{3,10} with $\omega_r \approx 6 \times 10^6 \text{ sec}^{-1}$ destabilizes when the average beam density throughout the column reaches a threshold value³ ($n_b/n_0 \gtrsim 0.001$) and propagates with the same azimuthal velocity as the beam. The mode is a standing wave in both the parallel and radial directions. Before reaching the nonlinear stage, the instability grows in time with the growth rate predicted by linear warm-plasma theory.

Figure 1 shows the growth and saturation of the lower-hybrid instability for different beam densities but constant beam energy and temperature. In Fig. 1(a) the instability monotonically approaches a constant saturation level in a few growth times ($\sim 100 \mu\text{sec}$), which is consistent with the quasilinear diffusion-time estimate for the measured wave amplitude, $e\bar{\varphi}_{\text{max}}/T_0 \approx 0.08$. With high-

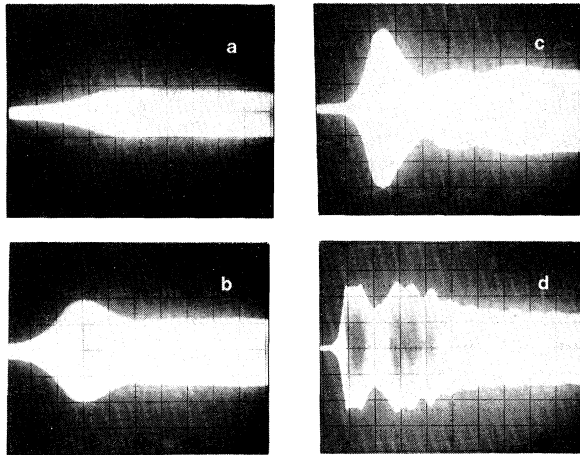


FIG. 1. Instability evolution for various beam densities. $n_0 = 10^9 \text{ cm}^{-3}$; $u_{b\perp}/v_0 = 5.4$; $T_b = 0.5 \text{ eV}$. All time scales are $20 \mu\text{sec/div}$. (a) $\bar{n}_b/n_0 = 0.18\%$, $e\bar{\varphi}/T_0 = (0.1)/\text{div}$; (b) 0.27% , (0.1) ; (c) 0.45% , (0.2) ; (d) 2.4% , (0.4) .

er beam densities and growth rates, the amplitude overshoots in Figs. 1(b) and 1(c) are not consistent with a slowly developing stochastic process; they represent the beginning of a trapping cycle as the instability leaves the quasilinear regime. The maximum amplitude of the overshoot $\bar{\varphi}_{\text{max}}$ is often 2–3 times the steady-state level, up to $e\bar{\varphi}_{\text{max}}/T_0 \sim 1$. The potential fluctuation $\bar{\varphi}$ is measured with calibrated Langmuir and capacitively coupled probes (with accuracy of $\sim 20\%$).³

In Fig. 1(d), where spectral measurements show two modes of high growth rate, wave-wave interactions become an important nonlinear effect. After the overshoot of the fastest growing wave, the second wave ($\gamma_2 < \gamma_1$) can suddenly detrap ions from the main wave, and the reappearance of random-phase interactions allows a quasilinear-like plateau to be formed,¹¹ in good agreement with particle simulation results.¹²

The coherence of a wave is determined by its autocorrelation time [$\tau_{ac} \approx 1/\Delta\omega$ or more strictly defined by the phase velocity spread, $\tau_{ac} = (\bar{\mathbf{k}} \cdot \delta\bar{\mathbf{v}}_p)^{-1}$], which has to be compared to the linear growth time ($\tau_g = \gamma^{-1}$), bounce frequency for a trapped particle [$\tau_b = 2\pi/\omega_b = 2\pi(M_i/e\bar{\varphi}k^2)^{1/2}$], and the beam's velocity-space diffusion time [$\tau_d \approx (\delta v_p)^3 / [2(e/M)^2 \sum k \bar{\varphi}_k^2]$]. The requirements for quasilinear theory to be valid are $\gamma \ll \omega_r$ and $\tau_{ac} < \tau_g < \tau_d$, while trapping becomes important when $\tau_b < \tau_g < \tau_{ac}$. These time scales are shown versus wave amplitude in Fig. 2 for the present beam-plasma parameters. Roughly speaking, if $\tau_g > \tau_{ac}$ the growth and saturation of the instability will

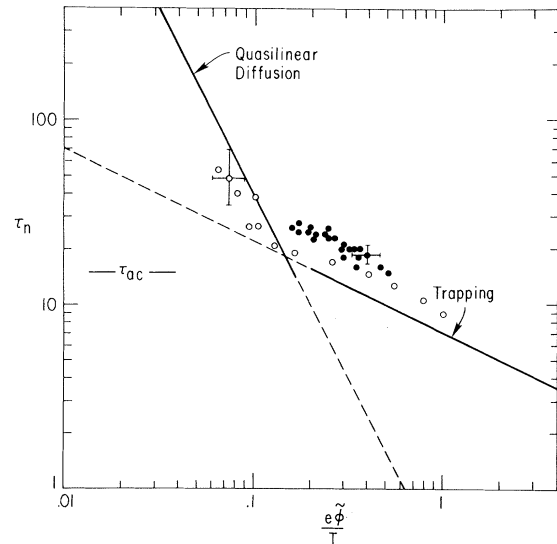


FIG. 2. Quasilinear diffusion and trapping times vs wave potential amplitude. All times are normalized to $\tau_p = 2\pi/\omega_{pi} (\approx 1 \mu\text{sec})$. $\tau_{ci} \approx 5\tau_{pi}$; $\tau_{ac} \approx 15\tau_{pi}$. Open circles are the nonlinear growth times, and closed circles are from fall times after the overshoot.

proceed as described by quasilinear theory on the time scale, $\tau_n \approx \tau_d \propto \bar{\varphi}_{\text{max}}^{-2}$. For $\tau_g \leq \tau_{ac}$, quasilinear theory is invalid, and eventually the wave saturates by trapping and slowing the beam; the time scale for the nonlinearity is then $\tau_n \approx \tau_b \propto \bar{\varphi}_{\text{max}}^{-0.5}$. The solid lines in Fig. 2 indicate the valid nonlinearity time scales. The open circles are the measured nonlinear growth times which are defined here as the time interval from the cessation of linear growth to saturation; the data show the expected transition at the same wave amplitudes at which the overshoots seen in Fig. 1 began.

The nonlinearity in the saturated state of the instability is largely determined by the initial linear excitation mechanism. In the quasilinear regime, Fig. 1(a), with the injection of a low-density warm beam the maximum wave growth is predominantly determined by inverse Landau damping [$\gamma \propto f'_b(\omega/k)_{\text{max}} \propto n_b/n_0$; $\gamma < \Delta\omega$]. With higher beam density, the growth rate of the wave with phase velocity $\omega/k \approx u_b [1 - 1/2(n_b/n_0)^{1/3}]$ becomes large mainly due to reactive coupling to satisfy $\gamma > \Delta\omega$.³ In the latter case, particle trapping causes wave saturation after the amplitude reaches the value to fulfill $(2e\bar{\varphi}/m)^{1/2} \approx u_b - \omega/k$ [Figs. 1(c) and 1(d)]. These characteristics are in agreement with those of O'Neil and Malmberg¹³ who define a beam-thermalization parameter $S = (v_b/u_b)(2n_0/n_b)^{1/3}$, where v_b is the beam's veloc-

ity spread; if $S < 1$ reactive coupling dominates, while for $S > 1$ resonant effects prevail. The present experiments were performed in the transition region $S \approx 0.2-5$.

To strengthen the association of the overshoot with trapping, the fall time (τ_f) is plotted as a function of $\tilde{\varphi}_{\max}$ in Fig. 2, and good agreement with the trapping relation $\tau_b \propto \tilde{\varphi}^{-1/2}$ is found. The appearance of a strong bounce frequency modulation is usually observed only for one bounce cycle after the initial growth; a coherent trapping oscillation tends to be suppressed because the trapped beam ions in different spiral steps oscillate with different phases in the potential trough of this flute-type ($k_z = 0$) wave. After the overshoot, we note, the wave frequency shifts to a slightly lower value ($\Delta\omega/\omega_{LH} < 0.1$) and the spectral width increases.

Ion distribution functions $f(v_{\perp})$ are measured with a small Faraday cup (size 2 mm; grid-collector spacing ≤ 0.2 mm) and boxcar sampling techniques with a resolution time of $2 \sim 4 \mu\text{sec}$. Because the instability propagates perpendicularly, it has no effect on the parallel component of the beam velocity. The time evolution of the perpendicular velocity distribution is shown in Fig. 3. In this case, the instability overshoot is weak and the time scale for the nonlinear modification of the distribution, $\tau_n \approx 15 \mu\text{sec}$, agrees with the time estimate from quasilinear diffusion for $e\tilde{\varphi}_{\max}/T_0 \approx 0.2$ which falls in the transition region, $\tau_n \approx \tau_d \approx \tau_b$. The beam distribution actually becomes monotonically decreasing before settling down to a level plateau, an effect also observed in particle simulations.¹² For lower beam densities (the quasilinear regime), accurate $f_b(v_{\perp})$ measurements could not be made because of the

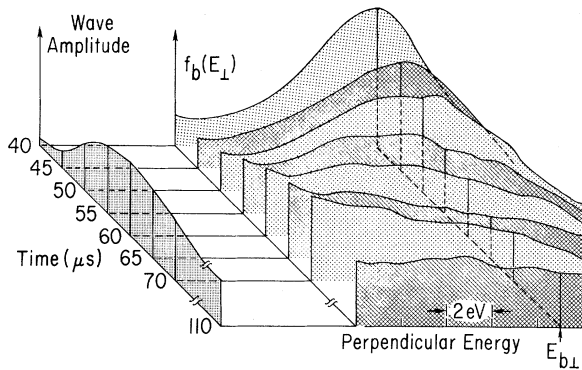


FIG. 3. Beam perpendicular energy distribution and wave amplitude vs time. For clarity, the target ion distribution is not shown. $e\varphi_{\max}/T_0 \approx 0.2 \pm 50\%$.

sensitivity of the energy analyzer.

Figure 4 gives an example of the evolution when the overshoot is stronger ($e\tilde{\varphi}_{\max}/T_0 \approx 0.3$) and a bounce back of the instability amplitude occurs. The distribution remains peaked until $\tilde{\varphi}$ reaches a maximum and then rapidly flattens. As the amplitude reaches a minimum, the peak reappears and slides to lower energy as the wave regrows. Although, this process occurs on a little longer time scale than trapping, it represents the partially reversible coherent oscillation of beam ions in wave troughs. (The whole process occurs in less than the beam transit time.)

The quasilinear theory for a two-dimensional

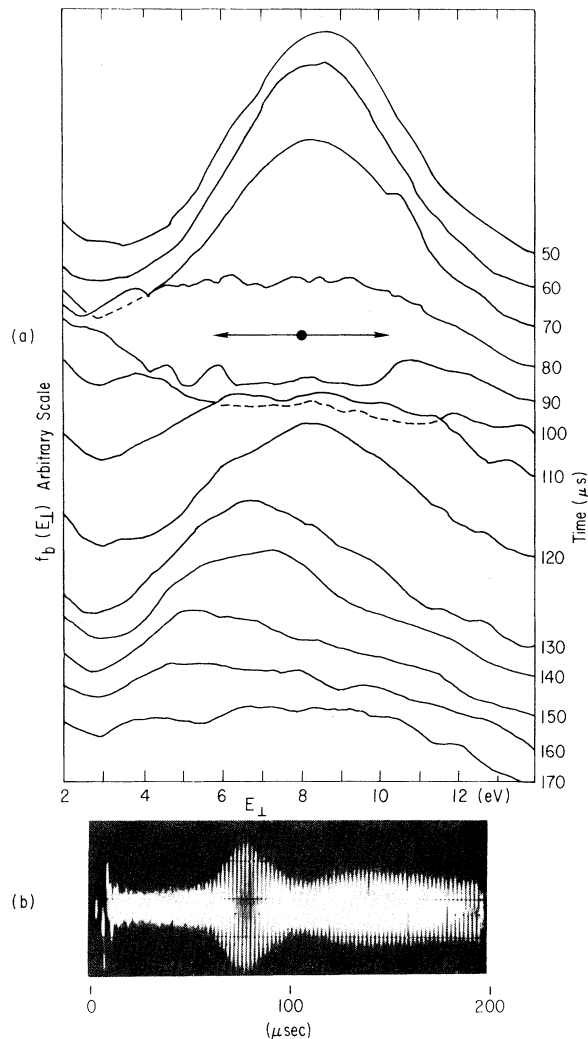


FIG. 4. (a) Beam perpendicular energy distribution and (b) wave amplitude vs time for $e\tilde{\varphi}_{\max}/T_0 \approx 0.3 \pm 50\%$ and a large initial overshoot. $(\frac{1}{2})mu_{b\perp}^2 = 8 \text{ eV}$. The arrow shows rough energy scale of the trapping width around $\frac{1}{2}m(\omega/k_{\perp})^2$ at $t \approx 80 \mu\text{sec}$.

ring or loss-cone distribution^{4,14} also suggests the occurrence of an overshoot, although the predicted amplitude dependence is $\tau_f \approx \bar{\varphi}^{-2}$ instead of $\tau_f \propto \bar{\varphi}^{-1/2}$ as observed here. In addition, the present geometry is effectively one-dimensional because both the beam and wave propagate along the same azimuthal path.³

As the instability grows and diffuses the beam in velocity space, it also diffuses the beam radially inward; as the beam ions slow in perpendicular velocity, their Larmor radii are reduced. This effect is observed as a flattened radial beam density profile after instability saturation. Wave heating of the target plasma was too small to be detected for reasons stated earlier.³

The anomalous beam slowing ($\nu_{\text{eff}}/\nu_{\text{classical}} \approx 10^2 - 10^3$) observed in the present experiment may have a strong impact on perpendicular neutral-beam injection in tokamak or mirror-fusion devices whenever a double-humped perpendicular ion velocity distribution occurs. In the preheating stage this anomalous effect may be useful, but it will have deleterious effects on the ripple injection scheme,¹⁵ or on the deuteron injection burning stage because of the rapid loss of fusible ions. In future fusion devices, high-energy charged fusion-reaction products (H, T, He³, He⁴) may also destabilize the lower-hybrid wave.¹⁶ These ions may be poorly confined because of their large banana orbits, and anomalously fast perpendicular momentum loss would be beneficial as it would improve the confinement of these particles.

Discussions with Dr. P. J. Barrett, Dr. H. Ikezi, Dr. P. K. Kaw, Dr. M. N. Rosenbluth, Dr. T. H. Stix, Dr. W. Tang, and Dr. S. Yoshikawa have been very valuable. We also thank

L. Gereg for his expert technical assistance. This work was supported by U. S. Energy Research and Development Administration Contract No. EY-76-C-02-3073.

¹H. L. Berk *et al.*, Nucl. Fusion **15**, 819 (1975).

²H. E. Mynick *et al.*, Phys. Fluids **20**, 606 (1977); J. A. Krommes *et al.*, to be published.

³S. Seiler *et al.*, Phys. Rev. Lett. **37**, 700 (1976); S. Seiler, Ph.D. dissertation, Princeton University, 1977 (unpublished).

⁴V. M. Kulygin *et al.*, Plasma Phys. **13**, 111 (1971).

⁵W. E. Drummond *et al.*, Phys. Fluids **13**, 2422 (1970); T. M. O'Neil *et al.*, Phys. Fluids **14**, 1204 (1971).

⁶K. W. Gentle and J. Lohr, Phys. Fluids **16**, 1464 (1973).

⁷W. E. Drummond and D. Pines, Nucl. Fusion, Suppl., Part 3, 1049 (1962); A. A. Vedenov *et al.*, Nucl. Fusion, Suppl., Part 2, 465 (1962).

⁸K. W. Gentle and C. W. Roberson, Phys. Fluids **14**, 2780 (1971).

⁹M. Yamada *et al.*, Phys. Fluids **20**, 450 (1977).

¹⁰J. M. Macbride *et al.*, Phys. Fluids **15**, 2367 (1972), and references therein; R. C. Davidson and N. T. Gladd, Phys. Fluids **18**, 1327 (1975).

¹¹M. Seidl *et al.*, Phys. Fluids **19**, 78 (1976).

¹²R. L. Morse and C. W. Nielson, Phys. Fluids **12**, 2418 (1969); D. Biskamp and H. Welter, Nucl. Fusion **12**, 89 (1972).

¹³T. M. O'Neil and J. M. Malmberg, Phys. Fluids **11**, 1754 (1968).

¹⁴R. C. Davidson, *Methods in Nonlinear Plasma Theory* (Academic, New York, 1972), Chap. 9.

¹⁵D. L. Jassby and R. J. Goldstone, Nucl. Fusion **16**, 613 (1976).

¹⁶L. P. Mai and W. Horton, Jr., Phys. Fluids **18**, 356 (1975).

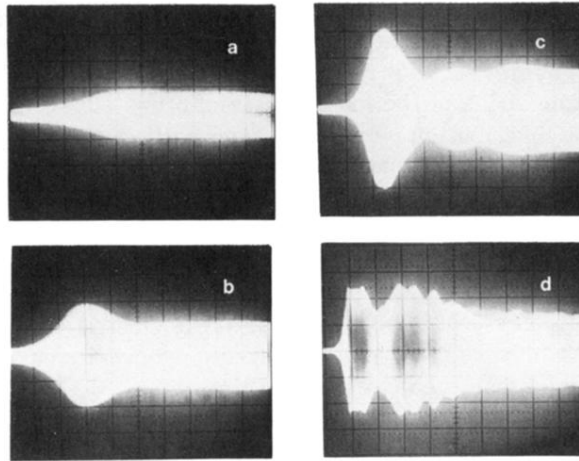


FIG. 1. Instability evolution for various beam densities. $n_0 = 10^9 \text{ cm}^{-3}$; $u_{b\perp}/v_0 = 5.4$; $T_b = 0.5 \text{ eV}$. All time scales are $20 \mu\text{sec}/\text{div}$. (a) $\bar{n}_b/n_0 = 0.18\%$, $e\tilde{\varphi}/T_0 = (0.1)/\text{div}$; (b) 0.27% , (0.1) ; (c) 0.45% , (0.2) ; (d) 2.4% , (0.4) .

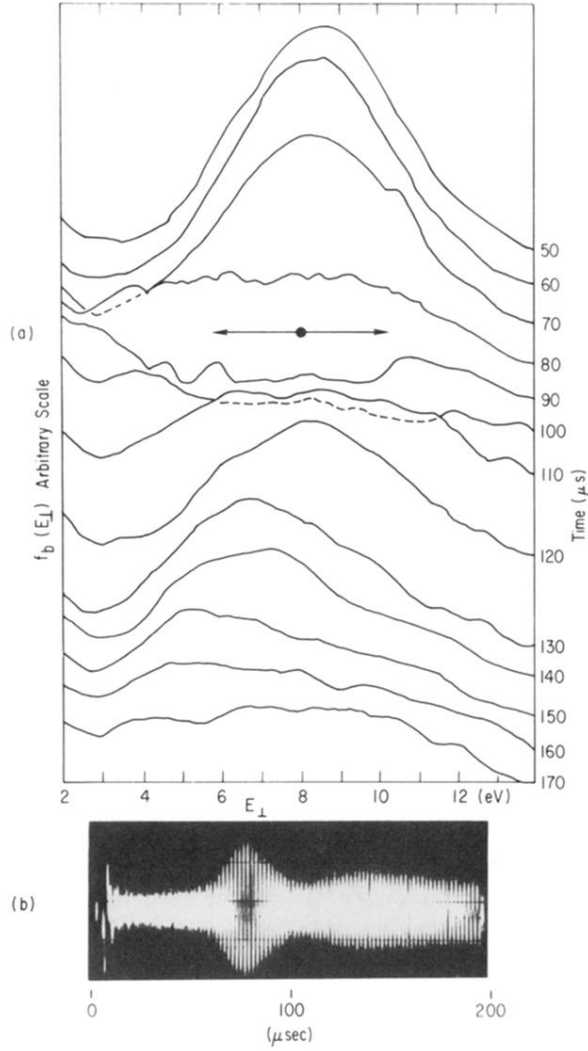


FIG. 4. (a) Beam perpendicular energy distribution and (b) wave amplitude vs time for $e\tilde{\varphi}_{\text{max}}/T_0 \simeq 0.3 \pm 50\%$ and a large initial overshoot. $(\frac{1}{2})mu_{b\perp}^2 = 8$ eV. The arrow shows rough energy scale of the trapping width around $\frac{1}{2}m(w/k_{\perp})^2$ at $t \simeq 80$ μsec .